Cell, Vol. 76, 901–912, March 11, 1994, Copyright © 1994 by Cell Press

Meiotic Chromosome Pairing in Maize Is Associated with a Novel Chromatin Organization

R. Kelly Dawe,* John W. Sedat,† David A. Agard,† and W. Zacheus Cande*
*Department of Molecular and Cell Biology
University of California
Berkeley, California 94720
†Department of Biochemistry and Biophysics
and Howard Hughes Medical Institute
University of California, San Francisco
San Francisco, California 94143

Summary

Three-dimensional light microscopy and the excellent cytological features of maize meiotic chromosomes are used to analyze the early events of chromosome synapsis. We demonstrate that the chromosomes undergo a dramatic structural reorganization prior to synapsis in zygotene. The unique features of prezygotene chromosomes are a partial separation of sister chromatids, an elongation of knob heterochromatin, an increase in surface complexity, a 50% increase in total chromosome volume, and a peripheral localization and alignment of telomeric, but not proximal, loci. At zygotene, chromosome volume decreases and chromosomes appear as single fibers. The specialized prezygotene chromosome morphology may facilitate homology recognition once the homologs have been brought together.

Introduction

Meiosis is a complex and specialized cell division that is required in the formation of germ cells to ensure that diploid cells give rise to viable haploid gametes. The most critical events of meiosis occur during the first prophase, when homologous chromosomes recognize and pair with each other. At the onset of prophase I, the sister chromatids condense into a specialized leptotene chromosome, in which the sister chromatids are held close together. The homologous chromosomes are then brought into rough alignment during zygotene, and a side-by-side synapsis begins. In the pachytene stage, the chromosomes become completely paired along their length and are bound together by a fibrous periodic array called the synaptonemal complex. The successful completion of chromosome synapsis facilitates genetic recombination and ultimately ensures that one copy of each chromosome is distributed to each of the four daughter cells (Loidl, 1990). Although many aspects of chromosome pairing are under debate (Maguire, 1988; Loidl, 1990), one of the most controversial issues is the relationship of recombination to synapsis (Hawley and Arbel, 1993). The traditional view holds that chromosomes must synapse before they recombine (Rhoades, 1961; John, 1990), but recent data from yeast demonstrate that the earliest steps in recombination precede synapsis (Kleckner et al., 1991; Goyon and Lichten, 1993).

Part of the confusion in understanding chromosome pairing lies in our current inability to reconcile cytological and molecular descriptions of the process. A primary question in cytological research is how chromosomes move through the nucleus and pair with each other. Although no consensus has been reached, many authors believe that chromosomes are first brought together via their telomeres, which bind to the nuclear envelope and frequently cluster together in zygotene (reviewed by von Wettstein et al., 1984). Such observations have led to models that involve a cytoplasmic force generation system that, by interacting with chromosomes through the nuclear envelope, draws chromosome ends together (e.g., Salonen et al., 1982). However, it is unclear whether telomere clustering is a precondition or a consequence of the general pairing and alignment that occur in zygotene (Loidl, 1990). In fact, chromosomes without telomeres seem to pair normally (reviewed by Maguire, 1984), suggesting that if telomeres actively congregate to initiate pairing, their role is indirect or catalytic.

Many of the genes that encode recombination enzymes in yeast have been cloned and characterized (reviewed by Hawley and Arbel, 1993). The phenotypes of mutants in the recombination pathway indicate that the molecular events required for recombination also provide the homology recognition used for pairing (reviewed by Kleckner et al., 1991). Time course studies further indicate that recombination in yeast begins at a time when the chromatin is diffuse and occupies most of the nucleus (Padmore et al., 1991; Goyon and Lichten, 1993). Based on these observations, it has been suggested that once stable contacts between chromosomes are established, the process of chromosome pairing could be driven by the force of chromatin condensation (Kleckner et al., 1991). In support of this hypothesis, in situ hybridization to yeast chromosomes was used to show that the chromosomes appear to align during the process of condensation (Scherthan et al., 1992). This contrasts with data from a variety of plant and animals species in which serial electron microscopy suggests that the already condensed leptotene chromosomes are not obviously aligned (Moens, 1969; Gillies, 1975; Holm, 1977a; Jenkins, 1983).

A thorough understanding of the relationship between states of chromatin condensation and chromosome pairing will necessarily involve high resolution studies of chromatin structure during meiotic prophase. Maize is uniquely suited for this purpose because of the excellent cytology of the male meiocyte as well as the large body of literature that has accumulated from years of intensive study (Carlson, 1988). The male meiocyte in maize contains large meiotic chromosomes that can be distinguished based on length, centromere position, and characteristic heterochromatic elements (Rhoades, 1950). Knobs, which are large blocks of heterochromatin found at specific sites,

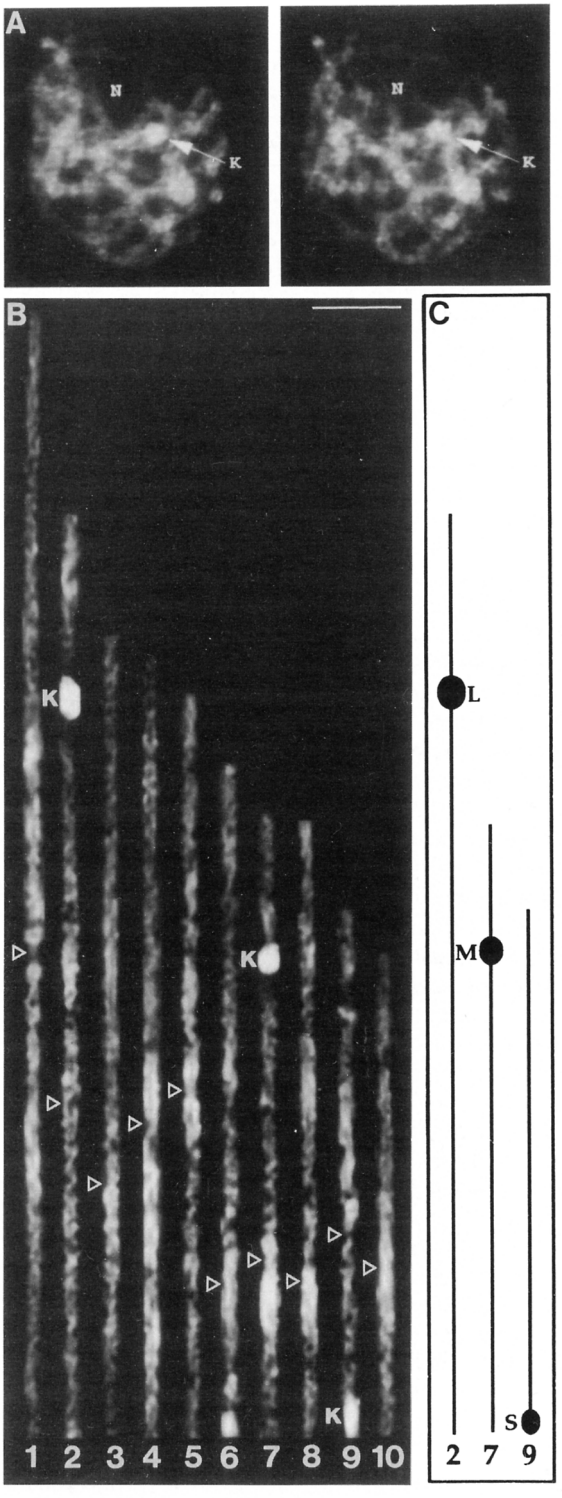

Figure 1. Pachytene Karyotype of the Inbred Line A665

(A) An A665 cell in pachytene presented as a stereo pair of a three-dimensional data set.

(B) Chromosomes within three-dimensional data stacks were computationally straightened (see Experimental Procedures; one of the two cells used is shown in [A]). Each chromosome is oriented with the small arm down, and the chromosome number is indicated below. The approximate location of the centromeres was determined by comparison to published photographs (e.g., Rhoades, 1950) and denoted with open triangles. The positions of the large knob on chromosome 2L, the medium-sized knob on 7L, and the small knob on 9S are noted (K). Scale bar, 5 μm.

(C) Schematic of chromosomes 2, 7, and 9, showing location and size of knobs. L, large; M, medium; S, small.

have been used in a number of seminal studies on chromosome behavior during meiosis (e.g., Creighton and McClintock, 1931). At least 28 maize mutants have been used to analyze nearly every aspect of meiosis, including mutants that affect the entrance and exit of meiosis, various aspects of synapsis and synaptonemal complex formation, metaphase chromosome structure, and spindle formation (e.g., Carlson, 1988; Golubovskaya, 1989; Staiger and Cande, 1990). In addition, the availability of transposon-tagging strategies (e.g., Han et al., 1992) will make it possible to combine molecular, cellular, and cytogenetic analyses of higher eukaryotic meiosis in a single experimental organism.

We have monitored chromosome morphology and distribution throughout early meiotic prophase using three-dimensional optical microscopy and a computerized epifluorescence light microscope workstation (Hiraoka et al., 1991). The unique cytological features of maize chromosomes have allowed us to correlate a complex series of chromatin rearrangements with the onset of pairing. We demonstrate that pairing is initiated immediately prior to zygotene, coincident with a global structural reorganization of the chromatin. The results are inconsistent with models of pairing that rely on premeiotic alignment of chromosomes or on chromosome condensation to bring homologous chromosomes together. Rather, we argue that the active movement of chromosomes and a specialized chromatin and nuclear architecture are critical elements of the early stages of pairing.

Results

Three-Dimensional Cytology of the Maize Meiocyte

The biology of male flower development in maize makes it readily possible to identify and characterize the stages and substages of meiosis. The male meiocytes develop within anthers, which are borne in the large terminal inflorescence called the tassel. Developmental gradients are found on each branch of the tassel, with the oldest flowers positioned toward the tip of the branch. Within these gradients, the size of the anther is correlated with the stage of meiosis (Chang and Nueffer, 1989), and each anther contains hundreds of meiocytes undergoing the early prophase stages in near-perfect synchrony (e.g., Staiger and Cande, 1990). A variety of maize inbred lines developed for agronomic purposes provide excellent material for meiotic studies. Although the inbred lines differ from each other in many characteristics, plants from a single inbred strain are highly uniform and can be assumed to be homozygous for virtually all genetic and cytogenetic markers.

We initially studied the pachytene stage of meiotic prophase I to determine whether we could reconstruct, using three-dimensional light microscopy, the same basic fea-

tures of the maize karyotype that have been established using squashed preparations. Anthers were dissected from their flowers and fixed with paraformaldehyde in a buffer designed to preserve chromatin structure (Belmont et al., 1987, and references therein). Following fixation, meiocytes were extruded and stained with the DNA-specific dye 4,6-diamidine-2-phenylindole dihydrochloride (DAPI), and optical sections were collected to create three-dimensional data sets. The stereo pair in Figure 1A illustrates that pachytene chromosomes are fully paired and well dispersed within the nucleus. Figure 1A also illustrates two major cytological features that were subsequently observed in all cells undergoing early meiotic prophase: a large nucleolus, which stains poorly with the DNA-specific dye DAPI, and deeply staining heterochromatic regions called knobs.

Knobs can be used to mark accurately specific regions of chromosomes at any stage of the cell cycle because they are constitutively condensed. Although relatively little is known about knob structure or function, all knobs contain an abundant, tandemly repeated 185 bp sequence (Peacock et al., 1981). Among the ten chromosomes of maize, knobs may occur at any of 21 specific positions (McClintock, 1978), but most commercial varieties of maize contain fewer than four knobs (e.g., Chughtai and Steffenson, 1989).

Figure 1B illustrates the pachytene karyotype of the A665 inbred line after the chromosomes were computationally straightened from three-dimensional data sets. (For the KYS inbred line, see Dawe et al., 1992.) The basic cytological features, including relative chromosome length, chromosome arm ratios, and the position of characteristic chromomeres, are very similar to that observed when specimens are prepared with acid–alcohol fixation and stained with carmine (Rhoades, 1950). For example, using either procedure, a series of heavily staining chro-

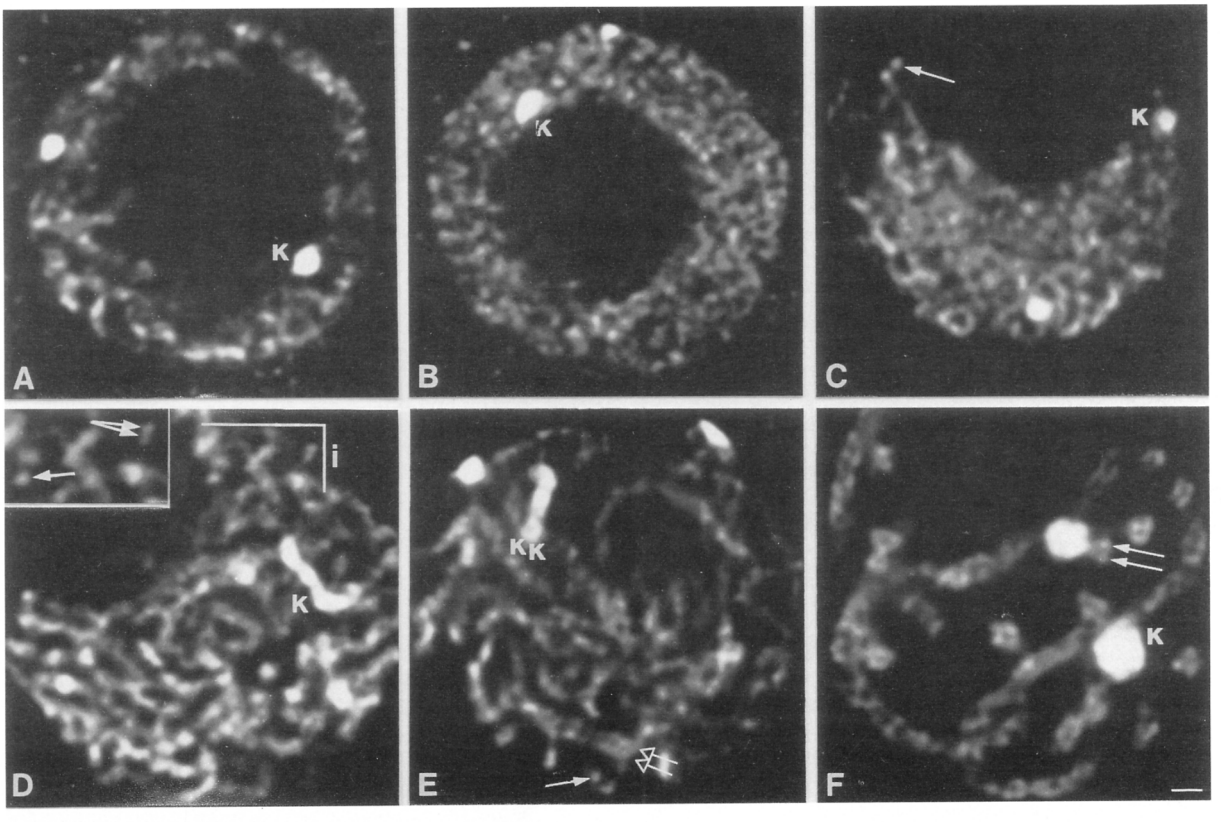

Figure 2. Optical Sections of Chromatin Morphology at Six Substages of Meiotic Prophase I

(A) Premeiotic interphase. The chromatin is diffuse and the large nucleolus is visible as a nonstaining region. The knobs (K) are spherical in shape.

(B) Early leptotene. Thin chromosomes are evident amid a diffuse background.

(C) Leptotene. All the chromatin is condensed and the knobs are unchanged and remain as spherical bodies. In cross section, the chromosomes appear circular (arrow). Each leptotene chromosome consists of two sister chromatids, but the sister chromatids cannot be distinguished from each other.

(D) Prezygotene. The chromosomes undergo a global structural reorganization. The inset at upper left shows a magnified view of the region indicated (i). Chromosomes either appear oval in cross section (arrow in inset) or split into two strands (forked arrow in inset). Unlike other stages of meiosis, the knobs are long and thin (K).

(E) Zygotene. Synapsed euchromatic regions are apparent (open arrows) and chromosomes are circular in cross section (arrow). Medium-sized knobs (K), still elongated, are seen as fully paired along their length.

(F) Pachytene. Chromosomes are fully synapsed and easily distinguishable. The knobs have returned to a spherical form. In cross section, paired cylindrical chromosomes are evident (arrows). Scale bar, 1 μm.

momeres is observed at the end of chromosome 4L (chromomeres are consistent features of the karyotype, with a characteristic staining intensity and location). There are also three differently sized knobs in the A665 inbred line: one very large knob on the long arm of chromosome 2 (2L), one medium-sized knob on 7L, and one small knob at the telomere of 9S. Our karyotype of the A665 inbred line differs from an earlier study, which placed the large knob on chromosome 7L and the medium-sized knob on chromosome 4L (Chughtai and Steffenson, 1989). Our ability to reconstruct the complete pachytene karyotype from optical sections illustrates that the maize meiocyte is readily accessible to study at the three-dimensional level. A more detailed analysis of pachytene chromosomes and the changes in morphology associated with the transition to diplotene will be the subject of another report.

Changes in Chromosome Structure during Meiotic Prophase I

We have undertaken a three-dimensional characterization of the cytological events of early prophase I as a first step toward understanding the process of chromosome pairing. Most of our studies were carried out on the A665 inbred line, but the basic structural events that lead to synapsis have been verified for the KYS and W23 inbred lines as well.

Chromosome pairing occurs within four substages of meiotic prophase I: premeiotic interphase, in which the chromosomes are diffuse and cannot be identified using traditional methods; leptotene, in which the chromosomes have condensed into thin fibers; zygotene, in which the chromosomes have begun to pair; and pachytene, in which all the chromosomes are fully synapsed and bound together by the synaptonemal complex. Gradual transitions make it possible to identify intermediate stages, and in our analysis we will ultimately identify and discuss six stages that precede pachytene. We will use pairing to describe a close association of homologs and will use synapsis only in the context of a tight pairing conditioned by the synaptonemal complex.

Our data on the structural aspects of pairing are presented as single optical sections in Figure 2, with relevant statistics on selected stages shown in Table 1. In the premeiotic interphase, the chromatin is uncondensed except for the large heterochromatic knobs, which are spherical in shape (Figure 2A). The subsequent stage is leptotene, which is the longest stage of meiotic prophase I in maize (approximately 43 hr; Hsu and Peterson, 1981). Owing to the significant amount of growth that occurs during this period, the early and late stages of leptotene can be readily distinguished by anther size (Table 1). The beginning stages of leptotene are characterized by newly formed strands amid diffuse background staining. This stage, which we define as early leptotene, is illustrated in Figure 2B. The next stage is the leptotene stage, in which all the chromatin is condensed the knobs remain as spherical bodies and the euchromatin is organized as discrete cylindrical fibers (Figure 2C). Although DNA replication has occurred by this stage (personal communication from C. Cronenwett and M. P. Maguire, 1967) and each leptotene chromosome actually consists of two sister chromatids, the sister chromatids cannot be distinguished from one another.

Table 1. Fiber Width and Knob Measurements

Measurement	Leptotene	Prezygotene	Zygotene
Fiber width[a]	0.32 ± 0.02	0.34 ± 0.03	0.34 ± 0.02
Small knob[b]	0.63 ± 0.13	1.57 ± 0.32	1.75 ± 0.28
Medium knob[b]	0.92 ± 0.10	3.14 ± 0.52	3.34 ± 0.27
Large knob[b]	1.11 ± 0.09	4.59 ± 0.60	4.40 ± 0.41
Size of anther[c]	1.25 mm	1.50 mm	1.75 mm

Chromatin measurements are presented in micrometers ± SD (n = 10 cells).

[a] At each stage the effective pixel size of half of the measured cells (five) was 0.07447 μm, and in the other half the pixel size was 0.06578 μm (see Experimental Procedures). Fiber width measurements in prezygotene were made on the smallest dimension of chromosomes when viewed in optical cross section. The differences in fiber width are not statistically significant.

[b] Measurements are of knob diameter (leptotene) or knob length (prezygotene and zygotene). For cells in leptotene and prezygotene, all six knobs were measured (n = 20 for each knob). Only one measurement was made when knobs were synapsed in zygotene (n = 11 for small knobs, n = 11 for medium knobs, and n = 12 for large knobs). The small, medium, and large knobs are significantly different in size at all stages ($P < 0.01$). All knobs are significantly larger in prezygotene and zygotene than they are in leptotene ($P < 0.01$).

[c] Approximate size of the anthers in the inbred line A665 that contain meiocytes in the stage indicated.

Immediately prior to synapsis, the chromosomes undergo a global structural reorganization. This newly identified stage of meiosis, identified by its characteristic chromosome morphology, will be called prezygotene. In prezygotene the chromosomes appear wider than in leptotene. The increase in width produces an oval-shaped chromosome in cross section, which can often be resolved into two distinct units (forked arrows in inset of Figure 2D). These observations suggest that there is a slight separation of the chromatids in prezygotene. When the prezygotene chromosomes were measured along their smallest dimension, they were roughly the same size as the leptotene chromosomes (Table 1; the values of 0.32 μm in leptotene and 0.34 μm in prezygotene were not significantly different). In addition, the previously spherical knobs become thin and distended during the prezygotene stage (Figure 2D). Relative to their length in leptotene, the knobs increased in length by 2.5- to 4.1-fold, depending on the original diameter of the knob (Table 1). Unlike previous stages in which the nucleolus is often excluded from the edge of the nucleus by intervening chromosomes, in prezygotene the nucleoli are invariably found at the nuclear periphery.

The extended knob morphology in prezygotene reveals considerable substructure that is not apparent during other stages. As shown in Figure 3, the large knob in A665 could be divided into three domains, a large central domain and two flanking domains of unequal size. We were able to use this characteristic asymmetry to determine the orientation of the large knobs and, by association, their

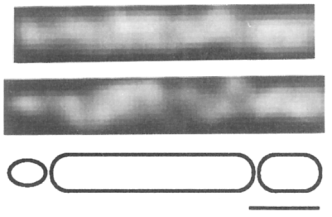

Figure 3. The Substructure of the Large Knob in A665

Above are two straightened chromosome 2L knobs from different prezygotene cells (see Experimental Procedures). Below is a schematic illustrating that when elongated, the large knobs invariably have a sharp end (left) and a blunt end (right) separated from a heterogeneous central region. Scale bar, 1 μm.

flanking chromatin during prezygotene (see following section).

Following prezygotene, the meiocytes enter the zygotene stage, during which the homologous chromosomes are incompletely paired along their length. During this period the chromosomes once again appear single and circular in cross section (see Figure 2E). The zygotene knobs, however, remain in their elongated state, with the relative dimensions similar to those observed in prezygotene (Table 1). The completion of chromosome pairing is evident in the pachytene stage. At this stage the sister chromatids are indistinguishable, and the knobs have returned to a spherical shape (see Figure 2F).

The Relationship between Chromatin Morphology and Chromosome Pairing

A significant though controversial body of literature suggests that chromosomes may be prealigned prior to the onset of meiosis (reviewed by Loidl, 1990). In addition, a recently proposed model suggests that as chromosomes condense, the homologs may be drawn closer together (Kleckner et al., 1991). Empirical tests of such models are limited by the fact that it is difficult to identify chromosomes until they are fully condensed. However, the constitutive heterochromatin of knobs is readily visible throughout meiotic prophase, and with the use of the A665 inbred line containing three differently sized knobs, it was possible to measure the physical relationships among the three loci at every stage. One of the knobs is on a telomere, and the two others are in midarm positions on different chromosomes (see Figure 1C). In the absence of pairing, the knobs should be distributed randomly relative to each other, whereas in cells with paired chromosomes, homologous knobs will be found closer to each other than to heterologous knobs.

Table 2 shows the mean distances between each of the homologous and heterologous knobs for cells in premeiotic interphase, early leptotene, leptotene, and prezygotene. In addition, Table 2 shows the percentage of knobs that were associated with the nuclear periphery (presumably the location of the nuclear envelope). The data provided no evidence for premeiotic alignment of chromosomes, since homologous knobs were not preferentially associated with each other in the premeiotic interphase. Nor was there any evidence that homologous knobs move closer together as the chromosomes condensed. Homologous knobs remained as distant from each other as they were from the heterologous knobs in early leptotene and leptotene (Table 2). These data demonstrate that chromosome pairing occurs after the chromosomes have completely condensed.

In prezygotene, the small knobs marking the telomeres on chromosome 9S became closely associated with each other (Table 2). The small knobs were always associated with the nuclear envelope (Table 2) and were very near the nucleolus (many 9S knobs were attached to the surface of the nucleolus and none were farther than 4.2 μm from its nearest edge). Although the small knobs were either close together or directly apposed to each other, the pairs of medium and large knobs remained as distant from each other as they were from their heterologous counterparts (Table 2). Only when the chromatin changed morphology in the zygotene stage were the medium- and large-sized

Table 2. Relative Knob Position during Early Stages of Meiotic Prophase

Measurement	Interphase	Early Leptotene	Leptotene	Prezygotene[a]
n	7	9	15	11
Small–small distance	6.13 ± 3.17	8.14 ± 2.68	7.26 ± 3.41	1.66 ± 1.65
Medium–medium distance	5.99 ± 2.68	7.87 ± 3.04	6.70 ± 3.31	7.41 ± 2.37
Large–large distance	7.34 ± 2.01	8.40 ± 3.02	7.95 ± 3.34	8.15 ± 3.1
Small–medium distance	6.53 ± 2.55	8.60 ± 3.17	8.17 ± 2.52	8.09 ± 2.72
Small–large distance	6.41 ± 2.76	9.12 ± 2.48	7.30 ± 3.22	8.30 ± 3.09
Medium–large distance	6.76 ± 2.52	7.37 ± 2.72	7.65 ± 2.79	7.15 ± 2.98
Percentage small on nuclear periphery	79	72	80	100
Percentage medium on nuclear periphery	36	61	50	14
Percentage large on nuclear periphery	86	83	67	41

Distances are measured in micrometers ± SD between the centers of small-, medium- and large-sized knobs. For the distances between heterologous knobs (small–medium, small–large, and medium–large), there were four measurements per cell. There were no significant differences among the knob distance data except in the prezygotene stage.

[a] There were highly significant differences among the prezygotene distance data ($P < 0.01$). When the small–small data were excluded from the analysis, there were no significant differences ($P > 0.3$). In 5 of the 11 cells in this group, the small knobs were directly apposed to each other. When those five cells were excluded from the analysis, significant differences in the distance data remained ($P < 0.05$).

knobs found in close association (for example, see Figure 2E).

Figure 4 illustrates stereo views of the homologous knobs in a single early leptotene cell and four prezygotene cells. As indicated by the quantitative data (Table 2), in early leptotene all the knobs appeared randomly placed (Figure 4A), whereas in prezygotene the small knobs became closely associated or directly apposed (Figures 4B–4E). Since the large knob assumes an asymmetrical configuration during prezygotene (see Figure 3), the relative orientation of this knob could be used to illustrate the presynaptic orientation of homologous regions on chromosome 2L. The homologous prezygotene knobs occurred in a variety of relative orientations, including roughly colinear, head to head, antiparallel, and offset (Figures 5B–5E, respectively). These data suggest that chromosome pairing is not facilitated by a preexisting alignment and

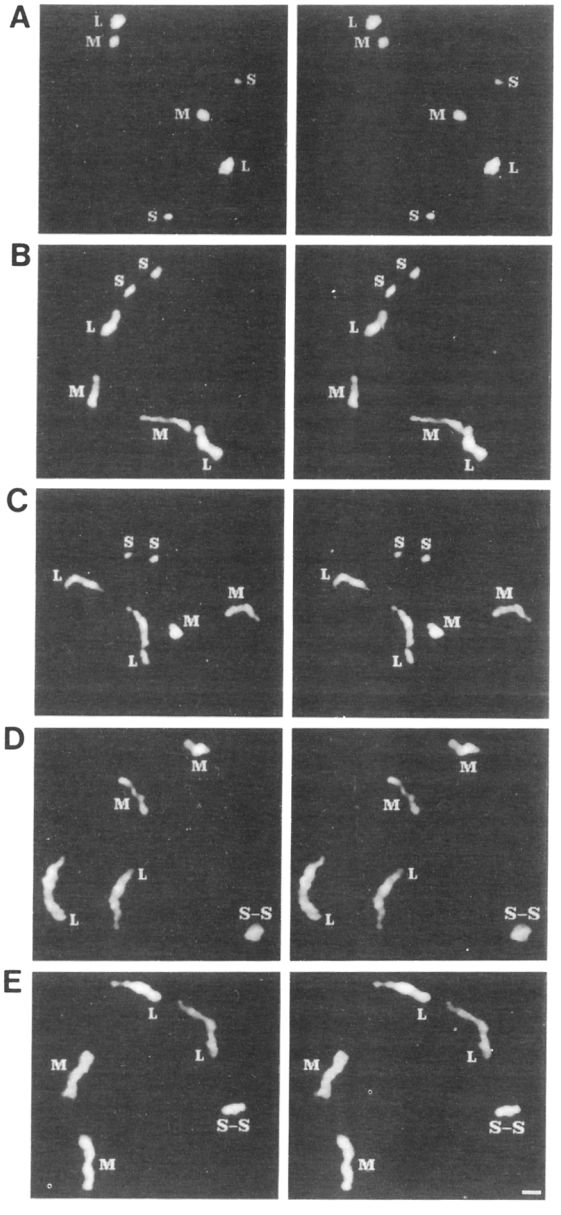

Figure 4. Knob Locations in Early Prophase I Cells

The images are stereo pairs that have been processed so that only the knobs are represented (see Experimental Procedures). The knobs are labeled S for the small knob on chromosome 9S, M for the medium-sized knob on chromosome 7L, and L for the large knob on chromosome 2L.

(A) An early leptotene nucleus. Note that the small knobs are widely separated.

(B–D) Prezygotene nuclei. In these cells the large knobs are labeled with an L at the blunt end of the knob (see Figure 3). In (C) and (D), the small knobs are apposed to each other and indicated as S–S. Scale bar, 1 μm.

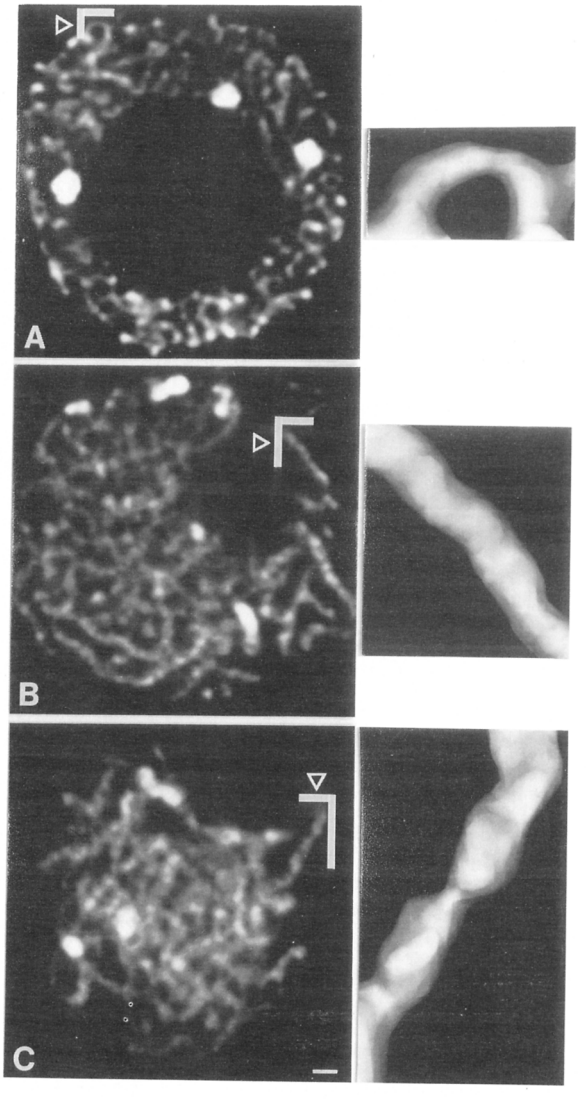

Figure 5. Stage-Specific Changes in Early Prophase I Chromosome Morphology

Each panel contains a single optical section (left) of the three-dimensional image that was used to prepare a solid model. Solid models (right) were constructed from several optical sections over the region of the image delimited by brackets (and indicated by arrowheads). (A) Leptotene. (B) Leptotene transition (between leptotene and prezygotene). (C) Prezygotene. Scale bar, 1 μm.

that a significant amount of chromosome movement must occur during zygotene for the chromosome 2L regions to be pulled into register.

The Nature of the Prezygotene Chromosome

During prezygotene, the knobs become distended, the euchromatic regions appear to enlarge, and the sister chromatids separate (see Figure 2D). The change from a leptotene to a prezygotene morphology is gradual, and intermediate stages can be identified by the presence of partially extended knobs. Cells that are in the transition between leptotene and prezygotene are at a stage we call leptotene transition. Figure 5 shows optical sections of a leptotene nucleus, a leptotene transition nucleus, and a nucleus in prezygotene. At the side of each optical section is a magnified solid surface image of a fiber within the cell, representing the contour of the chromosome surface. Surface renderings reinforce the impression that the chromosome increases in width during leptotene and further indicate that the transition to prezygotene increases the complexity of the chromosome surface.

The correlation between the prezygotene morphology and the earliest stages of chromosome pairing (Table 2) suggests that the novel chromatin architecture may be a precondition to the homology search. In principle, the transition to prezygotene could facilitate the homology search by reducing the distance between homologous chromosomes. If the chromosomes decondense, as suggested by their altered appearance (Figure 5), the effect could be to reduce the interchromosomal spaces and bring chromosomes closer together. However, this effect would only be significant if it occurred within the confines of a constant nuclear volume. A decondensation may also be correlated with a significant unraveling of the chromatin into the nuclear lumen, which could further enhance the opportunities for interaction between homologous sequences. An unraveling of the chromatin into the nuclear lumen would be detected as an increase in the DNA staining intensity between chromosomes.

Figure 6 illustrates a method for addressing these questions using established image-processing techniques (Russ, 1992), as implemented with the Prism program (Chen et al., 1989; see Experimental Procedures). Using a combination of computational filtering steps, nuclei were separated from cytoplasm (Figure 6B) and the chromosomes separated from the nuclear lumen (Figure 6C). The nuclear and chromosome "segmentation masks" (Figures 6B and 6C) were designed to exclude the nucleolus from the analysis. Using the appropriate masks, total volume and mean staining intensity levels were then calculated for both the chromosome and the nuclear lumen compartments. The quantitative data from leptotene, leptotene transition, prezygotene, and zygotene are illustrated in Figure 7.

As meiosis proceeds from leptotene to zygotene, total chromosomal volume increased from a low of 259 μm^3 in leptotene through a high of 395 μm^3 in prezygotene and subsequently back to an intermediate value of 316 μm^3 in zygotene (Figure 7A, $n = 7$ for each stage). Hence, in prezygotene the chromosomes occupied approximately 50% more space than in leptotene. In a related experiment, the volume of the large knobs in leptotene and prezygotene nuclei were calculated. The knobs also underwent a significant increase in volume of roughly 25%, indicating that the volume changes are not limited to the euchromatin (the mean ± SD combined volume of the two large knobs in leptotene was 2.35 ± 0.35 μm^3 and in prezygotene was 2.96 ± 0.56 μm^3, $n = 7$, $P < 0.05$). Additionally, we found that when the chromatin increased in volume during prezygotene, the nucleus itself also enlarged (Figure 7B). The nucleus and chromosomes appear to condense and decondense in unison; cells with large chromosomal volumes invariably have large nuclear volumes.

Staining intensity measurements within nuclei indicated that the amount of chromatin in the interchromosomal spaces was nearly constant throughout the pairing stages (Figure 7C). Although our intensity measurements would not detect a subtle or localized unraveling of the chromatin, it is clear that a wholesale decondensation of the chromatin into the nuclear lumen does not occur in either prezygotene or zygotene.

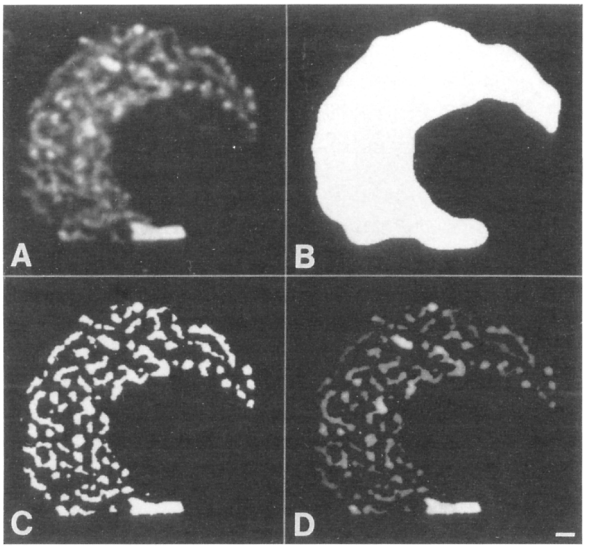

Figure 6. Segmentation Masks and a Masked Zygotene Image

The segmentation procedures are described in Experimental Procedures. (A) A single optical section of a zygotene starting image (dark-staining medium-sized knobs are partially synapsed). (B) Nuclear mask. (C) Chromosomal mask. (D) Starting image showing the chromosomes only, which was made by masking the cytoplasm and nuclear lumen.

Discussion

A Novel Chromatin Morphology Is Associated with the Pairing of Telomeres

This study represents a comprehensive description of early meiotic prophase I chromatin dynamics as they relate to the onset of pairing. Our study was facilitated by high resolution three-dimensional light microscopy methods

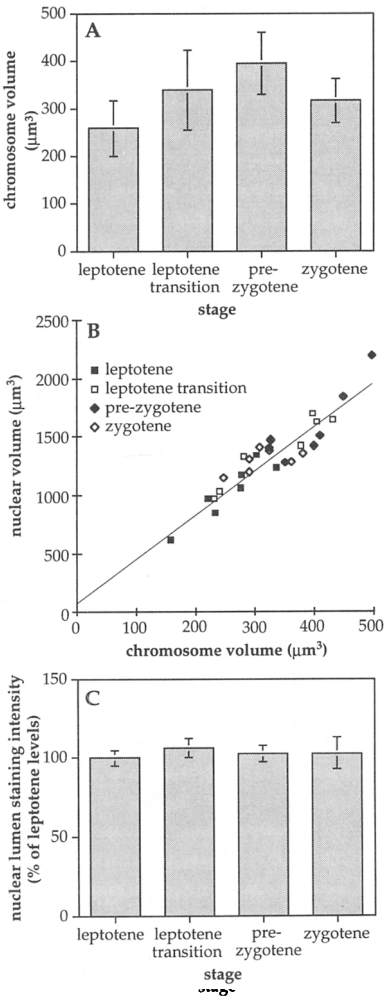

Figure 7. Chromosomal Volume and Nuclear Lumen Staining Intensity as a Function of Stage

(A) Chromosome volume. The values for leptotene and prezygotene are significantly different ($P < 0.01$), as are the values for prezygotene and zygotene ($P < 0.05$).

(B) Relationship between nuclear and chromosomal volume at different stages. The regression line shown has a coefficient of 3.78 ($P < 0.01$).

(C) Nuclear lumen staining intensity. The differences among the staining intensity data are not statistically significant.

Data in (A) and (C) were derived from the same 28 cells, where $n = 7$ for each stage and error bars indicate SD.

(Agard et al., 1989), which provide ease of data collection and the opportunity to apply powerful image processing techniques (Chen et al., 1989; Hiraoka et al., 1991; Russ, 1992). We have reaffirmed the long-standing view that the first condensation step in leptotene produces a highly condensed single fiber, in which the sister chromatids are tightly associated with each other (John, 1990). This initial condensation phase then gives way to a dramatic chromosome transformation in a stage we designate prezygotene. In prezygotene the chromatids separate slightly (Figure 2D), the surface complexity of the fiber increases (Figure 5), chromosome volume increases (Figure 7A), and the previously spherical heterochromatic knobs become long and thin (Figure 2D).

Although all of our studies were carried out in maize, elements of our observations are reflected in a number of other studies in which chromatin changes were observed during the process of pairing. In a study of the plant Bellevalia romana, a transition from single to double strandedness was demonstrated during the course of leptotene (Oehlkers and Eberle, 1957; see also Rhoades, 1961). Doubled leptotene chromosomes are also seen in the grouse locust Acridium granulatum, in the lily relative Fritillaria meleagris, and in the fungus Neotiella (Robertson, 1931; Huskins and Smith, 1934; Westergaard and von Wettstein, 1970). Changes in the appearance of heterochromatic elements during synapsis have also been reported. There are thin blocks of heterochromatin in the early leptotene chromosomes of lily that virtually disappear at the onset of pairing (Stern et al., 1975; Holm, 1977b). In the insect Phaulacridium vittatum, heteropycnotic B chromosomes become diffuse during zygotene, suggesting to the authors that such heterochromatic elements deheterochromatinize during synapsis (John and Freeman, 1975). The chromosomes of the fungus Coprinus loosen and elongate prior to synapsis (Lu and Raju, 1970), and a number of researchers using electron microscopy have noted that chromosomes appear to become more tightly condensed with the beginning of zygotene, as if the previous stage were slightly decondensed (maize [Gillies, 1975]; human [Bojko, 1983]; wheat [Jenkins, 1983]). Taken together, these observations indicate that the basic conclusions and implications of this study are relevant to a broad spectrum of higher eukaryotic organisms.

To investigate the relevance of chromatin structure to the onset of pairing, we utilized differently sized heterochromatic knobs as markers for chromosome position. We recognize that knobs do not represent an average euchromatic locus or even other heterochromatic regions. However, it is unlikely that knobs are inert homogeneous structures. The reproducible gaps and thick and thin regions in the elongated knobs (Figure 3) imply that knobs contain not only a repeated 185 bp element (Peacock et al., 1981) but a variety of other sequence elements as well. Even if the heterochromatic elements themselves do not initiate pairing, the observation that pairing in plants is generally initiated at a large number of evenly spaced sites along the chromosome (Maguire, 1985; Vincent and Jones, 1993, and references therein) indicates that knob behavior must be heavily influenced by flanking elements. The facts that each knob has its own affinity for the nuclear envelope (Table 2), that it only associates with its homolog, and that it pairs in a strictly stage-specific manner (Table 2) support the assertion that knobs are subject to the same general forces of pairing that govern euchromatin.

The maize inbred line A665 has three differently sized knobs, with the smallest lying close to the telomere of chromosome 9S (Figure 1C). Thus, by measuring the three-dimensional position of each homologous knob within a cell, we could not only relate pairing behavior to specific chromatin morphologies, but also relate the

pairing of telomeres to that of more proximal chromosomal regions. The chromosomes showed no indication of pairing until prezygotene. In every prezygotene cell, the homologous telomeres of chromosome 9S were significantly closer to each other than they were to the other homologous or heterologous knobs. In addition, the 9S telomeres were invariably attached to the nuclear envelope (Table 2) and close to the nucleolus. This observation agrees with the previous reconstruction of a single maize leptotene cell, which showed that at least 26 of the 40 telomeres had congregated within a small specialized region of the nuclear envelope adjacent to the nucleolus (Gillies, 1975).

The larger knobs in A665 were also used to reveal the paths and orientations of internal subregions of the prezygotene chromosomes. We found no propensity for the chromosomes to be cooriented in prezygotene, even though the telomeres had migrated together (Figure 4). The absence of discernable preorientation makes it unlikely that premeiotic chromosome arrangements play a role in aligning chromosomes (see discussion by Loidl, 1990). These observations also relate to long-standing models that implicate telomeres in the first stages of pairing. The belief that telomeres initiate pairing is based on the fact that telomeres are found clustered together in zygotene and that the synaptonemal complex is first observed near the ends of chromosomes (reviewed by von Wettstein et al., 1984). From the existing data, Loidl (1990) questioned whether telomere clustering should be thought of as a precondition for pairing, when telomere clustering could also be interpreted as the end product of a more general presynaptic alignment in zygotene. However, our evidence clearly indicates that in maize a pairing of at least one telomeric region precedes pairing in internal sites. This observation complements cytogenetic data (Burnham et al., 1972) and cytological data from zygotene cells (Maguire, 1982) that a tight synapsis in maize usually begins near the ends of chromosomes (although there is some initiation at internal sites; Gillies, 1975).

The behavior of telomeres and observations of chromosome oscillation and rotation during early prophase I (Parvinen and Soderstrom, 1976) suggest that pairing involves a significant amount of chromosome movement. It is difficult to capture a dynamic system using fixed specimens, and it remains possible that some movement or rearrangement occurred during the fixation process. Ultimately, to resolve the kinetics of pairing, it will be necessary to make time-lapse three-dimensional observations in living cells.

The Relationship between Chromosome Condensation and Pairing

One of the goals of this study was to test empirically the idea that chromosome condensation could itself promote chromosome pairing. Kleckner et al. (1991) have argued, based on a paper by Smithies and Powers (1986), that a homology search at the time when chromatin occupies most of the nucleus would obviate the need for chromosomes to move over long distances to make initial contacts. Once a homolog is identified, they argue, stable contacts could be established that constitute an early stage in the process of recombination. These primary contacts could then serve the purpose of holding the chromosomes together as the chromatin condenses during leptotene, thus driving the chromosomes into register. The simplest interpretation of this model would predict that as chromosomes condense, they would be brought into closer proximity. However, our analysis of the physical relationship of knobs during the gradual process of leptotene condensation indicates that as chromosomes condense, the chromosomes remain randomly distributed (Table 2).

Another possibility is that condensation contributes to chromosome movement at a later stage, such as immediately prior to zygotene. Indeed, our data demonstrate a partial decondensation in prezygotene, which is followed by a recondensation in zygotene (Figure 7A). However, for chromosome condensation to promote chromosome movement, chromosomes must be moved into closer proximity during the decondensed phase so that the recondensation can have a pulling effect. Distances between chromosomes could be reduced either by a balloon-like expansion of the chromosomes within a constant nuclear volume or by an unraveling of the chromatin into interchromosomal spaces, providing an interaction between otherwise distantly located chromosomes.

There is striking positive correlation between chromosome and nuclear volume during the early prophase stages: as the chromosomes increase in volume, the entire nucleus also enlarges (Figure 7B). This phenomenon will reduce or eliminate the effect that chromosome enlargement might have on bringing chromosomes closer together. Although we know of no similar observation in the literature on meiosis, a correlation between condensation state and nuclear volume has been observed in a number of other systems (Belmont et al., 1984, and references therein). To determine whether there was a general unraveling of the chromatin into the interchromosomal spaces, we also measured the quantity of DAPI staining material in the nuclear lumen at successive stages. The staining intensity levels were relatively constant between leptotene and zygotene (Figure 7C). Although our analysis would not have detected small variations in staining intensity, at no stage after the premeiotic interphase can the bulk of the chromatin be considered to be in a diffuse state. Thus, our analyses of chromosome morphology are not consistent with a model that relies on chromatin condensation to drive pairing. Since our data were derived exclusively from maize, it remains possible that chromosome condensation has a significant role in driving chromosome pairing in yeast.

The Relationship between Chromosome Movement and Pairing

A significant amount of chromosome movement is associated with pairing. Our data (Table 2) and previous studies (e.g., Thomas and Kaltiskes, 1976; Bojko, 1983) indicate that in higher eukaryotes, telomeres move from being widely dispersed to being closely associated prior to synapsis. We further demonstrate that when the 9S chromosome telomeres have paired, homologous nontelomeric

regions remain strikingly malaligned, showing that a substantial amount of additional chromosome movement must occur between prezygotene and zygotene. Other evidence that pairing is associated with chromosome movement comes from studies of meiosis in the rat, in which time-lapse photography reveals extensive chromosome movement during late leptotene and zygotene (Parvinen and Soderstrom, 1976; Salonen et al., 1982). Inasmuch as chromatin condensation itself is not likely to move chromosomes (at least in maize; see previous section), chromosome movement is probably generated by non-chromosomal forces, such as those generated by the cytoskeleton. It is possible that the microtubule array associated with the maize meiocyte nuclear envelope (Staiger and Cande, 1990) mobilizes telomeres (Table 2) or other chromomeres that are often found at the nuclear periphery (Maguire, 1982).

We favor the idea that an active process of chromosome movement during prezygotene (or an analogous stage) provides the mechanism for bringing otherwise distant chromosomes into close proximity. In maize, the interchromosomal space is strictly conserved throughout the pairing process (Figure 7B) and could facilitate chromosome movement within the nucleus. More intimate interactions among chromosomes would be enhanced by the morphology of the prezygotene chromosomes, which are characterized by a separation of chromatids, a general increase in volume, and an increase in overall surface complexity. Each of these features would effectively increase the surface area available for interaction with other chromosomes. Homology could be identified by a strand invasion mechanism (Smithies and Powers, 1986). A series of homologous contacts, the formation of the synaptonemal complex, or both would be expected to reduce the relative movement of homologous chromosomes and to promote further interaction among them. Although such a mechanism would ultimately effect complete synapsis, it would promote early pairing in distal regions because telomeres are brought together first.

Experimental Procedures

Preparation of Meiocytes

The inbred A665 line was obtained from the Corn Breeding Project (Department of Agronomy, University of Minnesota, St. Paul, Minnesota). Approximately 50 anthers were removed from florets and placed into 1 ml of buffer A (Belmont et al., 1987) and 0.35 M sorbitol. An equal volume of buffer A plus 0.35 M sorbitol containing 8% paraformaldahyde (diluted from a 16% solution of formaldehyde, EM grade in ampoules; Electron Microscopy Sciences) was added, bringing the final concentration to 4% paraformaldehyde. The petri dishes were placed on a shaker (120 rpm) at room temperature for 2 hr. Anthers were extensively washed with buffer A salts (buffer A without spermine, spermidine, or β-mercaptoethanol) and separated into groups by size (0.5, 0.75, 1.0, 1.25, 1.5, 1.75, and 2.0 mm). The end of each anther was removed using a fine scalpel, and the meiocytes were extruded using a forceps or tilted scalpel. Coverslips were prepared by acid washing for at least 2 hr in reagent-grade nitric acid, followed by extensive rinsing in water. Approximately 50 μl of 1 mg/ml polylysine (Sigma) was allowed to dry onto each coverslip. Meiocytes were transferred to the coverslips with a micropipettor (20–200 μl size), where they were allowed to settle to the surface. In one early experiment, the cells were spun down onto coverslips at 100 × g. While this step increased the adherence of cells to the coverslip, it was later found to cause an unacceptable level of cell flattening. For five following experiments, excess buffer was removed and the solution was allowed to evaporate until meiocytes could be seen on the surface (but before a salt residue was visible). At this stage the coverslips were placed in a 0.05 μg/ml solution of DAPI (Sigma) in buffer A salts for 10 min. Broken pieces of coverslip were placed at four corners on a slide, and a drop of 90% glycerol containing 100 mg/ml DABCO (1,4-diazobicyclo-(2,2,2)-octane; E. F. Fullam, Schenectady, New York) was added to the center. Coverslips were blotted to remove excess stain and placed upside down on the slide, and the edges were sealed with nail polish. Slides were stored in the dark at 4°C and data were collected within 3 days. After deconvolution (see below), the degree of cell flattening (if any) was calculated by comparing the mean x and y dimensions with the z dimension. Cells were not used unless the z dimension was greater than 80% of the mean x–y dimension (with the sole exception that 4 of the 35 cells used to calculate the mean fiber width and knob dimensions shown in Table 1 did not meet this criterion).

Microscopy

Three-dimensional data were collected using wide-field optical sectioning microscopy (Hiraoka et al., 1991). Two different Olympus OM1 inverted microscopes were used, both of which were equipped with a 60× NA1.4 oil immersion lens (Olympus, Incorporated). The use of one of the microscopes was granted by Dr. L. F. Reichardt. Spherical aberration was reduced by choosing an immersion oil with an index of refraction of 1.512. Data were collected on 12-bit charge-coupled device cameras by automatically stepping through the cells at 0.2 μm intervals. Owing to inherent lens variation and optical path differences within the microscopes, the effective pixel sizes were either 0.07447 or 0.06578 μm. Data stacks were usually 340 × 340 pixels and contained 70–90 optical sections. After data collection, the out-of-focus information in each data stack was removed using three-dimensional constrained iterative deconvolution (Agard et al., 1989).

Image Processing and Analysis

Chromosome Width

For fiber width measurements, it was necessary to define the edges of chromosomes. Using the Prism program (Chen et al., 1989), a one-dimensional intensity profile was taken over the fiber of interest. Width measurements were made directly on the plot profile at the halfway point from the tip to the base of the intensity peak over the fiber. For prezygotene, measurements were made exclusively on the shortest dimension of chromosome cross sections. Ten independent measurements were made within each cell, and the numbers were averaged.

Chromosome and Knob Straightening

The three-dimensional paths of each chromosome (pachytene) or knob (prezygotene) were interactively traced in Prism and recorded as a series of connected points. All the gray level data included within a defined radius around the modeled paths were used as the input for a chromosome straightening program (Chen et al., 1989), which presents the three-dimensional data as straight and flattened (projections). A median filter (box size = 3) was used to smooth the data. Two different cells were used to prepare the complete karyotype in Figure 1. The straightened knobs in Figure 3 were also subjected to local contrast enhancement (Peii and Lim, 1982).

Knob Size

The diameters of the the spherical knobs in leptotene cells were determined by averaging the x and y dimensions (using the same edge criterion as used in chromosome width measurements). The lengths of the knobs in prezygotene were determined by manually tracing the knobs in three dimensions using Prism (Chen et al., 1989), which calculates the length of the modeled path.

Distances between Knobs

The center of each knob was determined by measuring the knob in three dimensions. Distances between knobs were determined from center to center using Prism, which calculates the distances between any two points in a data set.

Stereo Views of Knob Position

The images in Figure 4 were prepared by reassigning pixels within knobs to a value of 1 and all other pixels to a value of 0. Projections separated by 10° were calculated to produce stereo pairs. In leptotene (Figure 4A), the knobs stain more intensely than any other chromatin, so the binary image could be created using a single threshold value.

However, in prezygotene, the gray levels within the knobs often dropped to within levels reached by other deeply staining chromatin. Therefore, for the prezygotene cells (Figures 5B–5E), an imperfect threshold was chosen that included all the knob heterochromatin as well as non–knob chromatin. The non–knob chromatin was manually blocked out within Prism, and projections were calculated from the modified data.

Solid Surface Images

The edges of the chromosomes were determined (see the section on chromosome width above), and the intensity value at the edge was used to define a contour over the surface. Artificial shading was applied as described previously (Chen et al., 1989; Paddy et al., 1990).

Segmentation of Images

Images were separated into their chromosome and nuclear lumen components using a scheme based on a previous report (Swedlow et al., 1993). Our procedure had the following five basic steps.

Step 1: Low Pass Filtration

A median filter (box size = 11) was first used to remove punctate staining that is typically observed in the cytoplasm (probably mitochondrial DNA). The median-filtered images were then convolved with a Fourier space gaussian-edged low pass filter where σ = 25 pixels. These steps have the effect of bringing out gross features, like the general outline of the nucleus.

Step 2: High Pass Filtration

To highlight the detail of the chromosomes, the starting images were also convolved with a Fourier space gaussian-edged high pass filter where σ = 33.3 pixels.

Step 3: Segmenting of the Nucleus from the Cytoplasm

On the low pass image (from step 1), a threshold was chosen at the largest value that included all of the chromatin in the nucleus. This threshold contained all of the nuclear lumen as well, but not the nucleolus. All pixels with a value higher than the threshold were subsequently used as a "mask" of the nucleus. Using this nuclear mask, all of the cytoplasmic pixels were excluded from the high pass image (from step 2).

Step 4: Segmenting the Chromosomes from the Nuclear Lumen

A threshold was determined on the cytoplasm-masked high pass image (from step 3), above which all data in the nucleus were assumed to be chromosomal. The value of the threshold was determined by matching the width of the chromosomes at the threshold to the measured width of the chromosome on the starting image (see the section on chromosome width above) at several locations. Pixels with values above the threshold were used to mask the chromosomes.

Step 5: Calculating the Volume and Intensity within the Masks

Chromosomal and nuclear volume were determined by computationally counting pixels in the appropriate segment of the image. The gray level data of the same pixels provided fluorescence intensity values. Nuclear lumen intensity was calculated as a fraction of the total intensity within the nucleus.

Knob Volume

In seven leptotene and prezygotene cells, the portions of the image around the two large knobs were cut out and analyzed as separate data stacks. Thresholds at the edge of the knobs were defined (using the same criterion used in the section on chromosome width above), and the volume was determined using masks (as described in steps 3–4 above).

Image Display and Photography

Because of the intensely staining knobs, it was often necessary to ignore much of the high intensity gray level data when displaying images. This had the effect of improving contrast within euchromatic chromosomes and overexposing knobs. Images were photographed with T-MAX 100 film and printed on Kodak Polycontrast III RC paper using a #0 Kodak Polymax filter.

Statistical Analysis

The knob distance data were analyzed by analysis of variance. In all other cases, pairwise comparisons for significance were made using t tests.

Acknowledgments

We thank H. W. Bass and J. R. Swedlow for helpful discussions, as well as M. Foss and M. Sevik for critically reading the manuscript. This research was supported in part by a National Science Foundation postdoctoral fellowship in plant biology to R. K. D., a grant from the National Institutes of Health (GM23238) to W. Z. C., and support by the Howard Hughes Medical Institute to J. W. S. and D. A. A.

Received October 6, 1993; revised December 2, 1993.

References

Agard, D. A., Hiraoka, Y., Shaw, P., and Sedat, J. W. (1989). Fluorescence microscopy in three dimensions. Meth. Cell Biol. *30*, 353–377.

Belmont, A., Kendall, F. M., and Nicolini, C. (1984). Three-dimensional intranuclear DNA organization *in situ*: three states of condensation and their redistribution as a function of nuclear size near the G1–S border in HeLa S-3 cells. J. Cell Sci. *65*, 123–138.

Belmont, A. S., Sedat, J. W., and Agard, D. A. (1987). A three-dimensional approach to mitotic chromosome structure: evidence for a complex hierarchical organization. J. Cell Biol. *105*, 77–92.

Bojko, M. (1983). Human meiosis. VIII. Chromosome pairing and formation of the synaptonemal complex in oocytes. Carlsberg Res. Commun. *48*, 457–483.

Burnham, C. R., Stout, J. T., Weinheimer, W. H., Kowles, R. V., and Phillips, R. L. (1972). Chromosome pairing in maize. Genetics *71*, 111–126.

Carlson, W. R. (1988). The cytogenetics of corn. In Corn and Corn Improvement, G. F. Sprague and J. W. Dudley, eds. (Madison, Wisconsin: American Society of Agronomy), pp. 259–344.

Chang, M. T., and Nueffer, M. G. (1989). Maize microsporogenesis. Genome *32*, 232–244.

Chen, H., Sedat, J. W., and Agard, D. A. (1989). Manipulation, display, and analysis of three-dimensional biological images. In The Handbook of Biological Confocal Microscopy, J. Pawley, ed. (Madison, Wisconsin: IMP Press), pp. 153–165.

Chughtai, S. R., and Steffenson, D. M. (1989). Knob constitution of inbred lines of maize (*Zea mays L.*) and its implications in maize breeding. Sabrao J. *21*, 21–26.

Creighton, H. B., and McClintock, B. (1931). A correlation of cytological and genetical crossing-over in *Zea mays*. Proc. Natl. Acad. Sci. USA *17*, 492–497.

Cronenwett, C., and Maguire, M. P. (1967). Incorporation of tritiated thymidine by microsporocytes in maize. Maize Genet. Coop. Newslett. *41*, 179–180.

Dawe, R. K., Agard, D. A., Sedat, J. W., and Cande, W. Z. (1992). Pachytene DAPI map. Maize Genet. Coop. Newslett. *66*, 23–25.

Gillies, C. B. (1975). An ultrastructural analysis of chromosomal pairing in maize. C. R. Trav. Lab. Carlsberg *40*, 135–161.

Golubovskaya, I. N. (1989). Meiosis in maize *mei* genes and conception of genetic control of meiosis. Adv. Genet. *26*, 149–192.

Goyon, C., and Lichten, M. (1993). Timing of molecular events in meiosis in *Saccharomyces cerevisiae* stable heteroduplex DNA is formed late in meiotic prophase. Mol. Cell. Biol. *13*, 373–382.

Han, C. D., Coe, E. H., Jr., and Martienssen, R. A. (1992). Molecular cloning and characterization of *iojap* (*ij*), a pattern striping gene of maize. EMBO J. *11*, 4037–4046.

Hawley, R. S., and Arbel, T. (1993). Yeast meiosis and the fall of the classical view of meiosis. Cell *72*, 301–303.

Hiraoka, Y., Swedlow, J. R., Paddy, M. R., Agard, D. A., and Sedat, J. W. (1991). Three-dimensional multiple-wavelength fluorescence microscopy for the structural analysis of biological phenomena. Semin. Cell Biol. *2*, 153–165.

Holm, P. B. (1977a). Three-dimensional reconstruction of chromosome pairing during the zygotene stage of meiosis in *Lilium longiflorum (Thunb.)*. Carlsberg Res. Commun. *42*, 103–151.

Holm, P. B. (1977b). The premeiotic DNA replication of euchromatin and heterochromatin in *Lilium longiflorum (Thunb.)*. Carlsberg Res. Commun. *42*, 249–281.

Hsu, S.-Y., and Peterson, P. A. (1981). Relative stage duration of microsporogenesis in maize. Iowa State J. Res. *55*, 351–373.

Huskins, C. L., and Smith, S. G. (1934). Chromosome division and

pairing in *Fritillaria meleagris*: the mechanism of meiosis. J. Genet. *28*, 397–406.

Jenkins, G. (1983). Chromosome pairing in *Triticum aestivum cv. Chinese Spring*. Carlsberg Res. Commun. *48*, 255–283.

John, B. (1990). Meiosis (Cambridge, England: Cambridge University Press).

John, B., and Freeman, M. (1975). B-chromosome behaviour in *Phaulacridium vittatum*. Chromosoma *46*, 181–195.

Kleckner, N., Padmore, R., and Bishop, D. K. (1991). Meiotic chromosome metabolism one view. Cold Spring Harbor Symp. Quant. Biol. *56*, 729–743.

Loidl, J. (1990). The initiation of chromosome pairing: the cytological view. Genome *33*, 759–778.

Lu, B. C., and Raju, N. B. (1970). Meiosis in *Coprinus*. II. Chromosome pairing and the lampbrush diplotene stage of meiotic prophase. Chromosoma *29*, 305–319.

Maguire, M. P. (1982). Homologue pairing and synaptic behavior at zygotene in maize. Cytologia *48*, 811–818.

Maguire, M. P. (1984). The mechanism of meiotic homologue pairing. J. Theor. Biol. *106*, 605–615.

Maguire, M. P. (1985). Crossover frequencies within paracentric inversions in maize: the implications for homologous pairing models. Genet. Res. *46*, 273–278.

Maguire, M. P. (1988). Interactive meiotic systems. In Chromosome Structure and Function, J. P. Gustafson and R. Appels, eds. (New York: Plenum Press), pp. 117–144.

McClintock, B. (1978). Significance of chromosome constitutions in tracing the origin and migration of races of maize in the Americas. In Maize Breeding and Genetics, D. B. Walden, ed. (New York: John Wiley and Sons), pp. 159–184.

Moens, P. B. (1969). The fine structure of meiotic chromosome polarization and pairing in *Locusta migratoria* spermatocytes. Chromosoma *28*, 1–25.

Oehlkers, F., and Eberle, P. (1957). Spiralen und Chromomeren in der Meiosis von *Bellevalia romana*. Chromosoma *8*, 351–363.

Paddy, M. R., Belmont, A. S., Saumweber, H., Agard, D. A., and Sedat, J. W. (1990). Interphase nuclear envelope lamins form a discontinuous network that interacts with only a fraction of the chromatin in the nuclear periphery. Cell *62*, 89–106.

Padmore, R., Cao, L., and Kleckner, N. (1991). Temporal comparison of recombination and synaptonemal complex formation during meiosis in S. cerevisiae. Cell *66*, 1239–1256.

Parvinen, M., and Soderstrom, K.-O. (1976). Chromosome rotation and formation of synapsis. Nature *260*, 534–535.

Peacock, W. J., Dennis, E. S., Rhoades, M. M., and Pryor, A. J. (1981). Highly repeated DNA sequence limited to knob heterochromatin in maize. Proc. Natl. Acad. Sci. USA *78*, 4490–4494.

Peii, T., and Lim, J. S. (1982). Adaptive filtering for image enhancement. Opt. Eng. *21*, 108–112.

Rhoades, M. M. (1950). Meiosis in maize. J. Hered. *41*, 58–67.

Rhoades, M. M. (1961). Meiosis. In The Cell, Volume 3, J. Brachet and A. E. Mirsky, eds. (New York: Academic Press), pp. 1–75.

Robertson, W. R. B. (1931). Chromosome studies. II. Synapsis in the *Tettigidae*, with special reference to the presynapsis split. J. Morph. Physiol. *51*, 119–139.

Russ, C. R. (1992). The Image Processing Handbook (Boca Raton, Florida: CRC Press).

Salonen, K., Paranko, J., and Parvinen, M. (1982). A colcemid-sensitive mechanism involved in regulation of chromosomes during meiotic pairing. Chromosoma *85*, 611–618.

Scherthan, H., Loidl, J., Schuster, T., and Schweizer, D. (1992). Meiotic chromosome condensation and pairing in *Saccharomyces cerevisiae* studied by chromosome painting. Chromosoma *101*, 590–595.

Smithies, O., and Powers, P. (1986). Gene conversions and their relation to homologous chromosome pairing. Phil. Trans. Roy. Soc. (Lond.) B *312*, 291–302.

Staiger, C. J., and Cande, W. Z. (1990). Microtubule distribution in *dv*, a maize meiotic mutant defective in the prophase to metaphase transition. Dev. Biol. *138*, 231–242.

Stern, H., Westergaard, M., and von Wettstein, D. (1975). Presynaptic events in meiocytes of *Lilium longiflorum* and their relation of crossing over a preselection hypothesis. Proc. Natl. Acad. Sci. USA *72*, 961–965.

Swedlow, J. R., Sedat, J. W., and Agard, D. A. (1993). Multiple chromosomal populations of topoisomerase II detected in vivo by time-lapse, three-dimensional wide-field microscopy. Cell *73*, 97–108.

Thomas, J. B., and Kaltiskes, P. J. (1976). A bouquet-like attachment plate for telomeres in leptotene of rye revealed by heterochromatin staining. Heredity *36*, 155–162.

Vincent, J. E., and Jones, G. H. (1993). Meiosis in autopolyploid *Crepis capillaris*. I. Triploids and trisomics: implications for models of chromosome pairing. Chromosoma *102*, 195–206.

von Wettstein, D., Rasmussen, S. W., and Holm, P. B. (1984). The synaptonemal complex in genetic segregation. Annu. Rev. Genet. *18*, 331–413.

Westergaard, M., and von Wettstein, D. (1970). Studies on the mechanism of crossing over. IV. The molecular organization of the synaptonemal complex in *Neottiella (Cooke) Saccarado (Ascomycetes)*. C. R. Trav. Lab. Carlsberg *37*, 239–268.